Quantum field as a quantum cellular automaton: The Dirac free evolution in one dimension

Alessandro Bisio, Giacomo Mauro D'Ariano, Alessandro Tosini *

Dipartimento di Fisica dell'Università di Pavia, via Bassi 6, 27100 Pavia, Italy
Istituto Nazionale di Fisica Nucleare, Gruppo IV, via Bassi 6, 27100 Pavia, Italy

H I G H L I G H T S

- The free Dirac field in one space dimension as a quantum cellular automaton.
- Large scale limit of the automaton and the emergence of the Dirac equation.
- Dispersive differential equation for the evolution of smooth states on the automaton.
- Optimal discrimination between the automaton evolution and the Dirac equation.

A R T I C L E   I N F O

A B S T R A C T

We present a quantum cellular automaton model in one space-dimension which has the Dirac equation as emergent. This model, a discrete-time and causal unitary evolution of a lattice of quantum systems, is derived from the assumptions of homogeneity, parity and time-reversal invariance.

The comparison between the automaton and the Dirac evolutions is rigorously set as a discrimination problem between unitary channels. We derive an exact lower bound for the probability of error in the discrimination as an explicit function of the mass, the number and the momentum of the particles, and the duration of the evolution. Computing this bound with experimentally achievable values, we see that in that regime the QCA model cannot be discriminated from the usual Dirac evolution.

Finally, we show that the evolution of one-particle states with narrow-band in momentum can be efficiently simulated by a dispersive differential equation for any regime. This analysis allows for a comparison with the dynamics of wave-packets as it is described by the usual Dirac equation.

* Correspondence to: Dipartimento di Fisica dell'Università di Pavia, via Bassi 6, 27100 Pavia, Italy.
  E-mail address: alessandro.tosini@unipv.it (A. Tosini).

This paper is a first step in exploring the idea that quantum field theory could be grounded on a more fundamental quantum cellular automaton model and that physical dynamics could emerge from quantum information processing. In this framework, the discretization is a central ingredient and not only a tool for performing non-perturbative calculation as in lattice gauge theory. The automaton model, endowed with a precise notion of local observables and a full probabilistic interpretation, could lead to a coherent unification of a hypothetical discrete Planck scale with the usual Fermi scale of high-energy physics.

1. Introduction

The major problem of developing a quantum theory of gravity, whose effects should become relevant at the Planck scale, seems to require a deep reconsideration of the spacetime structure. Recently alternative models of spacetime are gathering increasing attention. We can cite for example the loop quantum gravity model by Rovelli, Smolin and Ashtekar [1–3], the causal sets approach of Bombelli et al. [4], the noncommutative spacetime of Connes [5], the quantized spacetime of Snyder [6], the doubly-special relativity of Camelia in [7,8] along with the deformed special relativity models of Smolin and Magueijo in [9]. Some of these approaches are even considered for experimental tests, see for example the recent experiment proposals by Hogan [10,11] and Brukner [12]. Moreover, the finiteness of the entropy of a black hole [13,14], which implies that the number of bits of information that can be stored is finite, has led to the idea that space–time at the Planck scale could be discrete and that the amount of information in a finite volume must always be finite.

In this work, following the ideas proposed in Refs. [15–19], we assume that at the Planck scale physical dynamics occurs on a discrete lattice and in discrete time steps. Considering for simplicity the one-dimensional case, the lattice is a chain of sites equally spaced with a period assumed to be equal to the Planck length ℓ_P, while a single time step is equivalent to a Planck time τ_P. Each site x corresponds to a quantum system whose dynamics is described by a *quantum cellular automaton* (QCA). The QCA generalizes the notion of cellular automaton of von Neumann [20] to the quantum case, with cells of quantum systems interacting with a finite number of nearest neighboring cells via a unitary operator describing the single step evolution.

One of the first theoretical notion of QCA appeared in Ref. [21], and later in [22,23] where it was referred to as linear quantum cellular automata, while the notion of QCA as a mean for simulating quantum physical systems originally appeared in Refs. [24–26]. Since then the QCAs have been a quantum-computer-science object of investigation with a rigorous formulation and relevant results about their general structure [27–29]. Moreover, in the field of quantum information, particular attention is devoted to the so-called *quantum walks* (QWs) which describe the quantum evolution of one particle moving on a discrete lattice and which correspond the one particle sector of QCAs with linear evolution [30–32].[1] This interest is motivated by the use of QWs in the design of quantum algorithms: in Ref. [33] Childs et al. proved that QWs provide an exponential speedup for an oracular problem and QWs are also known to provide polynomial speedups for many relevant problems [34–36].

The idea of modeling the physical evolution at the Planck scale on a discrete background first appeared in the work of 't Hooft [37]. However, in his work the automaton is classical, and it describes a deterministic discrete theory underlying quantum theory. Then the idea of using QWs for the simulation of Lorentz-covariant differential equations appeared in the pioneering works of Succi and

---

[1] Notice that in Ref. [30] the word quantum cellular automaton appears for the first time. However, the model presented in the paper describe the one-particle evolution and is technically a QW.

Benzi [38], Bialynicki-Birula [39] and in the context of lattice-gas simulations, especially in the works of Meyer [40] and Yepez [41].

It is important to stress that the approach we are proposing does not aim to a QCA-discretization of the known standard model of particle physics. Indeed, we do not want to determine the QCA dynamics by mimicking the known dynamics of Quantum fields but we propose to derive it from principles of symmetry and simplicity of the quantum algorithm. Clearly, because of the discreteness of this framework, the usual continuous symmetries (like the Poincaré invariance and the gauge symmetries) are no longer tenable and must be replaced. However, in the QCA model one can naturally require the invariance of the dynamics under the discrete symmetries of the lattice (like translation invariance, reflections and discrete rotations). In this work we consider a one dimensional QCA model which is linear[2] and which has the minimal number of internal degrees of freedom for a non-trivial evolution. We then show that it is possible to single out a class of unitarily equivalent QCA by imposing the symmetry under discrete translations, parity and time reversal. Among the QCA in this class, we then focus on the one whose expression reproduces the Dirac equation in the Weyl representation as a finite difference equation.

If the QCA model is a valid description of the microscopic dynamics, then it must recover the usual phenomenology of quantum field theory (QFT) at the energy scale of the current particle physics experiments. This means that the physics of the QCA model and the one of QFT must be the same as far as we restrict to quantum states that cannot probe the discreteness of the underlying lattice. It is then crucial to address a rigorous comparison between the QCA dynamics and the dynamics dictated by the usual Dirac equation at different energy scales. We address such a comparison as channel discrimination problem and we quantify the difference between the two evolution with the probability of error p_e in the discrimination. We derive a lower bound for p_e as a function of momentum, mass and number of the particles and the duration of the evolution. Computing this bound with experimentally achievable values, we see that automaton evolution is undistinguishable from the one given by the Dirac field equation. This result proves that, in the limit of input states with vanishing momentum, the QCA evolution recovers the Dirac equation. We notice that our analysis agrees with the works [42–46] that studied the continuum limit, i.e. when the lattice spacings and the time steps are sent to 0, of QWs in comparison with the Dirac or the Klein–Gordon equations.[3]

In order to gain insight about the kinematics described by the QCA model we focus on one-particle states that are smooth and have limited band in momentum. Their evolution can be approximated by a dispersive (momentum-dependent) differential equation whose features can be easily compared with the analogous expressions for the non-relativistic and relativistic cases. By using this tool we will then study an elementary discrimination experiment between the Dirac automaton evolution and the usual Dirac one based on particle fly-time.

The line of research suggested by this paper explores the possibility that quantum information processing underlies all of physics and is based on the principle, for the first time proposed by Feynman [48] and then refined by Deutsch [49], that every finite experimental protocol is perfectly simulated by a finite quantum algorithm. It is immediate to see that the principle implies both that the density of information is finite, and that the interactions are local. The discreteness of the automaton framework could also represent a possible way out of the typical problems affecting QFT originating from the continuous background that still lack a satisfactory interpretation (see [50–53]). For example, in a QCA model there cannot be ultraviolet divergences since the presence of a discrete lattice implies a cutoff in momentum. The QCA has an exact notion of observables, accommodates localized states[4] and measurements,[5] and is endowed with well defined probabilistic interpretation and could lead to a coherent unification of a hypothetical discrete Planck scale with the typical Fermi scale of high-energy

---

[2] Because of the linearity assumption one can regard this model as a second quantized version of a quantum walk.

[3] We would like also to point out Ref. [47], which appeared after the first version of the present paper, where the authors proved convergence of the solution of the QW to the solution of the Cauchy problem for the Dirac equation.

[4] Since the automaton evolution is strictly causal any local excitation remains local during the evolution.

[5] The relevance of presenting QFT as a probabilistic theory about local measurements has been also the main focus of the so called *algebraic quantum field theory* [54,55].

physics experiments. Finally, the field automaton is a physical model which is quantum *ab initio*, and is not derived by applying a quantization procedure to classical field theory.

It is worth emphasizing that the difference between the QCA approach and the discrete approach of lattice gauge theories is twofold. On the "foundational" side, our aim is to explore the idea whether it is possible to ground QFT on a more fundamental QCA theory, and then recover the usual quantum fields as a large scale approximation. Within this perspective, Lorentz covariance is supposed to hold only in the limit of small wave-vectors, whereas generally it is deformed [7–9,56] while approaching the Planck scale.[6] On a more "technical" side the evolution of the automaton is not given by a finite difference Hamiltonian or Lagrangian as in lattice gauge theory. The quantum automaton is based on a discrete and exactly causal unitary evolution and the Hamiltonian has no longer any physical relevance. The same fact that there is no Hamiltonian is the reason why the Fermion-doubling [58] is no longer an issue in the QCA framework (see e.g. [39]).

We conclude this introductory section with a short outline of the paper. In Section 2, after reviewing some generalities of QCAs and QWs, we discuss the covariance of a QCA with respect to the symmetry of the causal network and we derive a one dimensional linear QCA from the assumptions of minimal internal dimension, homogeneity, parity and time reversal invariance. In Section 3 we show how this automaton recovers the Dirac dynamics for small masses and momenta. Here, we set the problem by considering the probability of error p_e in the discrimination between the unitary channel corresponding to the automaton evolution and the one which corresponds to the evolution dictated by the Dirac equation. We obtain a lower bound for p_e in terms of the mass of the field, the number and the momentum of the particles, and the duration of the evolution. Then in Section 4 we present an analytical approximation method for evaluating the automaton evolution for one-particle states which are smooth in momentum and with limited bandwidth. Then we derive a dispersive (momentum-dependent) differential equation, which approximate the QCA evolution. We compare computer simulations with the analytic approximation, and provide the leading order corrections to the Dirac equation. After discussing possible ways of testing of the theory, like the effects of the automaton evolution on wave-packets fly-times, we conclude the paper with future perspectives.

2. The one-dimensional Dirac automaton

2.1. One dimensional field QCA and Quantum Walks

In this section, we present some generalities about QCA in one dimension and we review the notion of linear QCA and its connection with the one of Quantum Walk.

A one-dimensional QCA describes the discrete time unitary local evolution of quantum systems on the one-dimensional lattice $\mathbb{Z}$. Since we want to apply this model of evolution to quantum fields, any site $x \in \mathbb{Z}$ will correspond to a Bosonic or Fermionic quantum field operator $\psi(x)$ located at the same position. If the field has Λ internal degrees of freedom the operators

$$\{\psi_a(x)\}_{a \in A}, \quad A = \{1, \ldots, \Lambda\} \tag{1}$$

will denote the generators of the field local algebra $\mathcal{F}_x$ that satisfies the usual commutation, respectively anticommutation, rules $[\psi_a(x), \psi_b(x)]_{\pm} = [\psi_a^\dagger(x), \psi_b^\dagger(y)]_{\pm} = 0$, $[\psi_a^\dagger(x), \psi_b(y)]_{\pm} = \delta_{xy}\delta_{ab}$. The automaton corresponding to the one-step update of the field is required to preserve the above relation. In the usual QFT both the Fermionic and the Bosonic algebra's structure is preserved with the field evolving by a unitary operator U

$$\psi(x, t + 1) = U^\dagger \psi(x, t) U. \tag{2}$$

---

[6] In the explorative approach of this work we will describe the automaton dynamics in a fixed reference frame while the study of boosted automata and the features of the emerging spacetime have been the subject of another publication [57].
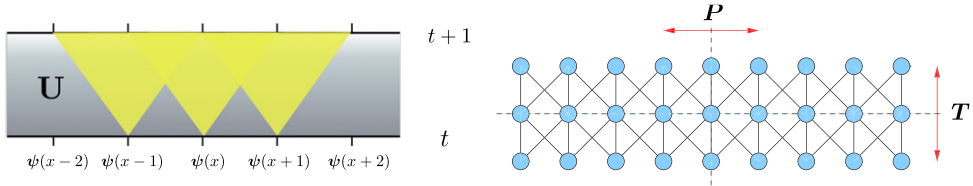
Fig. 1. Left figure: Illustration of a one-dimensional QCA unitary step. Each site of the lattice x corresponds to a quantum field evaluation $\psi(x)$. The field operator at site x interacts with the field $\psi(x \pm 1)$ at neighboring sites. In the case of the Dirac automaton the field operator has two components (see text). Right figure: Schematic of the three time steps causal network corresponding to a one-dimensional quantum cellular automaton with next-neighboring interaction. The topology of the network is left invariant by the mappings $x \mapsto -x$ and $t \mapsto -t$ and the dynamics of the automaton is assumed to be parity (**P**) and time reversal (**T**) invariant (see Eqs. (17) and (18)).

If we restrict to the evolution of free, i.e. non interacting, fields the evolution in Eq. (2) is linear in the field, namely we have

$$\psi_a(x, t+1) = \sum_{y \in \mathbb{Z}, \, b \in A} U^{ab}_{xy} \, \psi_b(y, t) \tag{3}$$

for some complex coefficients U^{ab}_{xy}. Upon introducing the vector field $\boldsymbol{\psi}$

$$\boldsymbol{\psi} := (\ldots, \psi(x), \psi(x+1), \ldots)^\top, \qquad \psi(x) := (\psi_1(x), \ldots, \psi_A(x))^\top, \tag{4}$$

where each $\psi(x)$ is also a vector with A components corresponding to the internal degrees of freedom of the field, we have the equality $\boldsymbol{\psi}(t+1) = \mathbf{U}\boldsymbol{\psi}(t)$ where $\mathbf{U}$ is the unitary matrix $\mathbf{U}\mathbf{U}^\dagger = \mathbf{U}^\dagger\mathbf{U} = I$ having entries U^{ab}_{xy} according to Eq. (3).

If we want the evolution of Eq. (4) to be local, $\psi(x, t+1)$ must be a linear combination of the field on few neighboring sites $\mathcal{N}_x \subset \mathbb{Z}$ at time step t, that is

$$\psi_a(x, t+1) = \sum_{y \in \mathbb{Z}, \, b \in A} U^{ab}_{xy} \, \psi_b(y, t), \quad U^{ab}_{xy} = 0 \,\, \forall y \notin \mathcal{N}_x. \tag{5}$$

The map $\mathbf{U}$ represents then a linear QCA with "cell structure" $\mathcal{F}_x$ and *neighborhood scheme* $\mathcal{N}_x$. In the following we consider automata with *nearest neighborhood scheme*, namely $\mathcal{N}_x = \{x-1, x, x+1\}$ (see left Fig. 1) (the next-neighboring interaction is not an assumption by itself, since it is always possible to reduce to such a case by grouping a periodic pattern of the network into a single node of the automaton) and satisfying *translational invariance*, say $\mathbf{U}$ must commute with the shift operator

$$[\mathbf{U}, S_1] = 0, \quad S_1 : \psi(x) \to \psi(x+1). \tag{6}$$

This implies that the only non zero entries of the matrix $\mathbf{U}$ are $\mathbf{U}_{y,y\pm1} = \mathbf{U}_{\pm1}$ and $\mathbf{U}_{y,y} = \mathbf{U}_0$ and that $\mathbf{U}$ has the simple band diagonal form

$$\mathbf{U} = \sum_{x \in \{-1,0,1\}} \mathbf{U}_x \otimes S_x = \begin{pmatrix} \ddots & \ddots & \ddots & & \\ & \mathbf{U}_{-1} & \mathbf{U}_0 & \mathbf{U}_1 & \\ & & \mathbf{U}_{-1} & \mathbf{U}_0 & \mathbf{U}_1 \\ & & & \mathbf{U}_{-1} & \mathbf{U}_0 & \mathbf{U}_1 \\ & & & & \ddots & \ddots & \ddots \end{pmatrix} \tag{7}$$

where the $\mathbf{U}_x$'s $A \times A$ are called *transition matrices*, while S_1, S_{-1}, S_0 correspond respectively to the right shift, left shift and the identity.

This framework is formally equivalent to a Quantum Walk on the Hilbert space $\mathbb{C}^A \otimes l_2(\mathbb{Z})$ with $\mathbb{C}^A$ the particle internal Hilbert space. A Quantum Walk is the generalization in the quantum framework of the common notion of random walk and it was introduced for the first time in Ref. [31] (for a review on QWs see e.g. Ref. [59] and references therein). It is known that a QCA restricted to the one-particle

sector corresponds to a QW. However, when the evolution is linear as in the present case, the one-particle dynamics fully specifies the evolution of many particles. By reversing the line of reasoning one can realize that a linear field-QCA is obtained by "promoting" the state $|\psi\rangle$ in the usual QW framework to a vector of field operators ψ (see the "second quantization" of a QW of Ref. [27]).

For convenience, as usual in the literature [32,59–62], we will study the dynamics of the field automaton in the momentum representation. For the field operator we have

$$\psi(k) := \frac{1}{\sqrt{2\pi}} \sum_{x \in \mathbb{Z}} e^{-ikx} \psi(x), \quad k \in [-\pi, \pi], \tag{8}$$

where with little abuse of notation we utilize the variable name k to denote the Fourier transform of any function of x. Notice that the automaton model is naturally band-limited $k \in [-\pi, \pi]$ and periodic in momenta due to the discreteness of the lattice. The automaton in the momentum space is then given by

$$\mathbf{U} = \int_{-\pi}^{\pi} dk \, \mathbf{U}(k) \otimes |k\rangle\langle k|, \qquad \mathbf{U}(k) = \sum_{x \in \{-1,0,1\}} \mathbf{U}_x e^{-ikx}, \tag{9}$$

and we can define the Hamiltonian $\mathbf{H}$ that describes the automaton evolution for continuous times, interpolating between time-steps, namely

$$\mathbf{H} = \int_{-\pi}^{\pi} dk \, \mathbf{H}(k) \otimes |k\rangle\langle k|, \qquad \mathbf{U}^t = \exp(-i\mathbf{H}t). \tag{10}$$

Upon diagonalizing the unitary $\mathbf{U}(k)$ we get the automaton one-particle eigenvalues and eigenvectors

$$u_k(s) = e^{-is\omega(k)}, \quad |s\rangle_k, \quad s = \pm, \tag{11}$$

with $\omega(k)$ the automaton dispersion relation.

The field automaton $\mathbf{U}$ generally operates on the vector field ψ which describes an arbitrary number of particles. The vacuum state for the automaton is defined as the state $|\Omega\rangle$ such that

$$\psi_s(k)|\Omega\rangle = 0 \quad \forall s = \pm, \; \forall k \in [-\pi, \pi]. \tag{12}$$

Up to now, we have not specified the nature Fermionic/Bosonic of the field. Here we will focus only on the Fermionic case of anticommuting field. A N-particle state can be obtained by acting with the field operator on the vacuum as follows

$$|N, \mathbf{k}, \mathbf{s}\rangle = \left(\prod_{i=1}^{N} \psi_{s_i}^{\dagger}(k_i)\right) |\Omega\rangle. \tag{13}$$

Specifically, for $N = 1$ particle eigenstates of $\mathbf{U}$, we write

$$\psi_s^{\dagger}(k)|\Omega\rangle = |s\rangle_k|k\rangle, \tag{14}$$

whereas for $N = 2$ we have $\psi_{s_1}^{\dagger}(k_1)\psi_{s_2}^{\dagger}(k_2)|\Omega\rangle = |s_1\rangle_{k_1}|s_1\rangle_{k_2}|k_1, k_2\rangle$ where $|k_1, k_2\rangle = -|k_2, k_1\rangle$, and so forth for $N > 2$. The corresponding eigenvalues of the (logarithm of) $\mathbf{U}$ are $\omega(N, \mathbf{k}, \mathbf{s}) = \sum_{i=1}^{N} s_i \, \omega(k_i, m)$.

2.2. Derivation of the one-dimensional Dirac automaton

In this section we present the derivation of simplest field automaton, here denoted Dirac QCA, that is covariant with respect to the symmetries of the one-dimensional causal network and that exhibits a non trivial evolution.

In general, the lattice of an automaton is endowed with certain discrete symmetries. The one-dimensional lattice $\mathbb{Z}$ only exhibits parity symmetry (see right Fig. 1), corresponding to the lattice reflection with respect to some site (and the time reversal symmetry if we consider the causal network

given by the automaton evolution). The invariance of the automaton dynamics with respect to a discrete symmetry of the lattice, given by a group G whose elements are linear functions $g : \mathbb{Z} \to \mathbb{Z}$, is satisfied if the QCA is *covariant* under a unitary representation $\{\mathbf{O}_g\}$ of G on the field local algebra $\mathbf{O}_g : \mathcal{F}_x \to \mathcal{F}_{g(x)}$, namely

$$\mathbf{U} = \sum_{x \in \{-1,0,1\}} \mathbf{O}_g \mathbf{U}_x \mathbf{O}_g^\dagger \otimes S_{g(x)}, \quad \forall g \in G. \tag{15}$$

In Appendix A we derive the simplest covariant one-dimensional automaton that exhibits a non-trivial (non-identical) evolution. We can summarize our assumptions as follows:

  (i) Unitarity of the evolution;
 (ii) Translation invariance;
(iii) Covariance under parity $x \mapsto -x$;
(iv) Covariance under time-reversal $t \mapsto -t$;
 (v) Minimal internal dimension Λ for a non-identical evolution.

The first two assumptions are already contained in the definition itself of translational invariant QCA which has the general form given in Eq. (7). From the band diagonal form of the unitary $\mathbf{U}$ it is immediate to see that the unitarity condition $\mathbf{U}\mathbf{U}^\dagger = \mathbf{U}^\dagger \mathbf{U} = I$ is equivalent to the following constraints on the transition matrices

$$\mathbf{U}_1 \mathbf{U}_1^\dagger + \mathbf{U}_{-1} \mathbf{U}_{-1}^\dagger + \mathbf{U}_0 \mathbf{U}_0^\dagger = I \qquad \mathbf{U}_0 \mathbf{U}_1^\dagger + \mathbf{U}_{-1} \mathbf{U}_0^\dagger = 0, \qquad \mathbf{U}_{-1} \mathbf{U}_1^\dagger = 0. \tag{16}$$

Assumptions (iii) and (iv) require the automaton to preserve the symmetries of the one-dimensional causal network (in right Fig. 1). The covariance for parity symmetry can be expressed as in Eq. (15) where the parity transformation $g(x) = -x$ has to be represented on the field local algebra via a unitary matrix $\mathbf{P}$ such that

$$\mathbf{U} = \mathbf{P}\mathbf{U}_1\mathbf{P}^\dagger \otimes S_{-1} + \mathbf{P}\mathbf{U}_{-1}\mathbf{P}^\dagger \otimes S_1 + \mathbf{P}\mathbf{U}_0\mathbf{P}^\dagger \otimes I. \tag{17}$$

Similarly, we impose the covariance for time reversal, which is not a symmetry of the lattice but of the full causal network, asking that

$$\mathbf{U} = (\mathbf{T} \otimes I)\mathbf{U}^\dagger(\mathbf{T}^\dagger \otimes I) = \mathbf{T}\mathbf{U}_1^\dagger\mathbf{T}^\dagger \otimes S_{-1} + \mathbf{T}\mathbf{U}_{-1}^\dagger\mathbf{T}^\dagger \otimes S_1 + \mathbf{T}\mathbf{U}_0^\dagger\mathbf{T}^\dagger \otimes I, \tag{18}$$

for some anti-unitary operator $\mathbf{T}$ (see Appendix A for the anti-unitarity of time reversal).

For $\Lambda = 1$ the only translational invariant QCA satisfying parity invariance is the identical one $\mathbf{U} = I$ (see Appendix A) as already proved by Meyer in the context of quantum lattice gases [40]. Next, we have the case $\Lambda = 2$. In this case we find (see Appendix A) that all the QCAs satisfying the conditions above are unitarily equivalent to the following automaton

$$\mathbf{U} = \begin{pmatrix} nS_{-1} & -im \\ -im & nS_1 \end{pmatrix}, \quad n, m \in \mathbb{R}^+, \ n^2 + m^2 = 1, \qquad \boldsymbol{\psi}(x) := \begin{pmatrix} \psi_L(x) \\ \psi_R(x) \end{pmatrix}, \tag{19}$$

where we named the two components of the field ψ_R and ψ_L *left* and *right* modes. Among the class of unitary equivalent QCAs, we have chosen the one whose expression reproduces the Dirac equation in the Weyl representation as a finite difference equation. The unitarity constraint $n^2 + m^2 = 1$ in Eq. (19) forces the parameter m to be $m \in [0, 1]$.[7]

In the momentum space (see Eq. (9)) the Dirac automaton is given by

$$\mathbf{U}(k) = \sum_{x \in \{-1,0,1\}} \mathbf{U}_x e^{-ikx} = \begin{pmatrix} ne^{ik} & -im \\ -im & ne^{-ik} \end{pmatrix}, \tag{20}$$

---

[7] We will see in the next section that in a certain limit the Dirac automaton evolution mimics the solutions of the Dirac evolution and the parameter m will play the role of the mass.
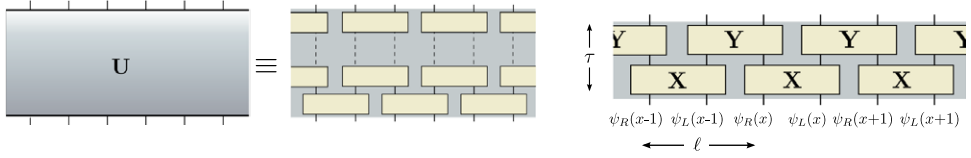
Fig. 2. Left figure: local implementation of the generic one dimensional automaton **U**. Right figure: the local implementation of the Dirac automaton (19) with $\mathbf{X} = -i\sigma_1$, $\mathbf{Y} = mI + in\sigma_1$.

and, upon its diagonalization, it is easy to derive the Hamiltonian of Eq. (10)

$$\mathbf{H}(k) = \frac{\omega}{\sin(\omega)} \begin{pmatrix} -n\sin(k) & m \\ m & n\sin(k) \end{pmatrix}, \tag{21}$$

with $\omega(k, m)$ the automaton dispersion relation

$$\omega(k, m) = \arccos(\sqrt{1 - m^2}\cos(k)). \tag{22}$$

In 1d we have that $\omega(k, m)$ is an increasing function of $|k|$, and then there is no Fermion doubling, namely no state other than for $k = 0$ corresponding to a minimum of the energy $\omega(k, m)$ (for dimension greater than one, the dispersion relation can be as well made monotonic continuous by exploiting the multi-valued nature of the dispersion relation [63], as pointed out in Ref. [39]). The eigenvalues and the eigenvectors of the unitary matrix $\mathbf{U}(k)$ in Eq. (20) are given by

$$u_k(s) = e^{-is\omega}, \quad |s\rangle_k := \frac{1}{\sqrt{2}}\begin{bmatrix} \sqrt{1 - sv} \\ s\sqrt{1 + sv} \end{bmatrix}, \quad s = \pm, \tag{23}$$

in terms of the automaton dispersion relation (22) and the group velocity $v = \partial_k\omega$.

As we will see in Section 4, in analogy with the Dirac theory, the eigenvalues with $s = 1$ in Eq. (23) correspond to positive-energy particle states, whereas the eigenvalues with $s = -1$ correspond to negative-energy anti-particle states. The most general state $|\psi\rangle$ is thus a superposition of a positive and a negative energy state, i.e. $|\psi_+\rangle + |\psi_-\rangle$, and typical aspects of the Dirac-field dynamics, such as the Zitterbewegung and the Klein paradox, are also dynamical feature of the Dirac automaton as shown by the authors in a more recent paper [64].

Notice that in the derivation of the automaton our assumptions imply a minimal internal dimension $\Lambda = 2$ for a non-identical evolution. This means that it is not possible to consider an automaton having just an internal degree of freedom—say a scalar field. Moreover, although it is not the focus of this work, it is interesting to notice that as a byproduct of the assumptions leading to the Dirac automaton we also have its localizability, namely the possibility of decomposing the unitary **U** in a number of more elementary gates involving only neighboring systems as shown in the left Fig. 2. This is the so-called Margolus scheme [65]. It is well known from the Cellular Automata and walks theory that the locality of the automaton does not ensure the existence of a local implementation (typical examples of local but non localizable automata are the right and left shifts, which do not satisfy parity). Werner et al. proved [29] that a necessary and sufficient condition for the localizability of a QW is that $\det(\mathbf{U}(k)) = $ const, where $\mathbf{U}(k)$ is the momentum representation of the walk. As already noticed the one-particle sector of the Dirac field automaton **U** coincides with a walk (see Eq. (7)) and we can exploit the above result. In the Dirac case it is $\det(\mathbf{U}(k)) = n^2 + m^2 = 1$ (see Eq. (20)) which shows the localizability of corresponding unitary evolution. Moreover, as shown by Arrighi et al. [28], a localizable d dimensional QCA can be locally implemented using 2^d layers of quantum gates and then by just two layers in the 1d case. For the one-dimensional Dirac automaton (19) we have the local implementation shown in the right Fig. 2 and the local gate **X** and **Y** are as follows [17]

$$\mathbf{X} = -i\sigma_1, \qquad \mathbf{Y} = mI + in\sigma_1. \tag{24}$$

3. Recovering the Dirac dynamics

By interpreting the parameters k and m of the Dirac automaton as momentum and mass, it is reasonable to expect that the usual kinematics of the Dirac equation

$$i\partial_t \boldsymbol{\psi}(k, t) = \mathbf{H}_D(k)\boldsymbol{\psi}(k, t) \quad \text{where } \mathbf{H}_D(k) = \begin{pmatrix} -k & m \\ m & k \end{pmatrix} \tag{25}$$

is recovered in the small momenta ($k \to 0$) and small mass ($m \to 0$) regime. More precisely, one would say that it is not possible to tell the difference between the automaton evolution $|\psi(t)\rangle = U_A^t |\psi(0)\rangle$ and the evolution given by Dirac Hamiltonian $|\psi(t)\rangle = U_D^t |\psi(0)\rangle$ (U_D^t is the unitary evolution given by the Dirac Hamiltonian) as far as the mass m is small and the momentum of initial state $|\psi\rangle$ is small. This idea can be rigorously recast in terms of a discrimination problem between two black boxes. The scenario can be described as follows. An experimentalist is given a black box that can be either the automaton (box A) or the usual Dirac equation (box D) with equal probability, and he is asked to guess which box. The most general experiment which discriminates between two unitary evolutions amounts to the following three steps procedure[8]: (i) preparing a quantum state ρ, (ii) apply the unknown unitary evolution U_X ($X = A, D$) (iii) perform a two outcome measurement on the output state: the two outcomes A and D correspond to the two possible evolutions. The measurement is described by a positive operator valued measure (POVM) $\mathbf{P} = \{P_A, P_D\}$, where P_A and P_D are positive operators on $\mathcal{H} \otimes \mathcal{K}$ which satisfy $P_A + P_D = I$, I denoting the identity. Then the probability of error reads

$$p_e(P_A, \rho) = \frac{1}{2}\text{Tr}[P_A((U_D \otimes I)\rho(U_D^\dagger \otimes I) - (U_A \otimes I)\rho(U_A^\dagger \otimes I))]. \tag{26}$$

It is clear from this scenario that the minimum of the probability of error over all the possible experiments is a well defined measure of how much the models A and D are far apart. Minimizing expression (26) over all the possible experiments entails a minimization over the set of the POVM's and the set of the available states. The minimization over the POVM set gives [67]:

$$\inf_{0 \le P_A \le I} p_e = \frac{1}{2} - \frac{1}{2}\|U_D\rho U_D^\dagger - U_A\rho U_A^\dagger\|_1 \tag{27}$$

where $\|\sigma\|_1$ denotes the trace norm $\|\sigma\|_1 = \text{Tr}[\sqrt{\sigma^\dagger \sigma}]$. If we now set bounds on the number of particles $N \le \bar{N}$ and their momentum $k \le \bar{k}$, the minimization over the admissible input states ρ is:

$$\bar{p}_e = \frac{1}{2} - \frac{1}{2}\sup_{\rho \in \mathcal{T}_{\bar{k},\bar{N}}} \|U_A\rho U_A^\dagger - U_D\rho U_D^\dagger\|_1, \tag{28}$$

where $\mathcal{T}_{\bar{k},\bar{N}}$ denotes the set

$$\rho \in \mathcal{T}_{\bar{k},\bar{N}} \quad \text{iff} \quad \text{Tr}[\rho N_{\bar{k}}] = \text{Tr}[\rho P_{\bar{N}}] = 0 \tag{29}$$

where $P_{\bar{N}}$ is the projector on the $N > \bar{N}$-particles sector and $N_{\bar{k}}$ is the operator that counts the number of particles with momentum $|k| > \bar{k}$, i.e. $N_{\bar{k}} = \int_{|k|>\bar{k}} dk\, \boldsymbol{\psi}^\dagger(k)\boldsymbol{\psi}(k)$.

In Appendix B we evaluate a lower bound for $\bar{p}_e$ probability of error, which is given by

$$\bar{p}_e \ge \frac{1}{2} - \frac{1}{2}\sqrt{1 - \cos^2(g(\bar{k}, m, \bar{N}, t))} \tag{30}$$

where

$$g(\bar{k}, m, \bar{N}, t) := \bar{N} \arccos\left(\cos(\bar{\alpha}t) - \bar{\beta}\right)$$
$$\bar{\alpha} := \max_{k \in \{0, \bar{k}\}} |\omega_D - \omega|, \qquad \bar{\beta} := \max_{k \in \{0, \bar{k}\}} \left|\frac{1}{2}\left(1 - vv_D - \sqrt{(1 - v^2)(1 - v_D^2)}\right)\right| \tag{31}$$

---

[8] In general, the optimal discrimination needs entangled states, but for the case of two unitary evolutions this is not necessary [66].
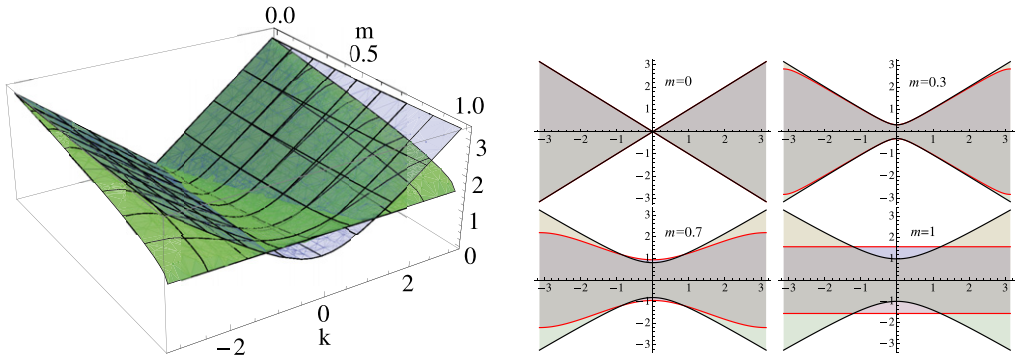
Fig. 3. Comparison between the dispersion relations $\omega(k, m)$ of the Dirac automaton and of the Dirac equation, in Eqs. (22) and (35), respectively. In the top figure the dispersion relation is plotted versus the adimensional mass $m \in [0, 1]$ and momentum $k \in [-\pi, \pi]$ ($m = 1$ corresponds to the Planck mass). The green surface represents the automaton, whereas the blue the Dirac one. In the bottom figures $\omega(k, m)$ is plotted versus k for four values of m (the red line corresponds to the automaton, whereas the black one is the Dirac's). We can see that the two dispersion relations coincide for small masses and momenta, and the larger the mass the smaller the overlap region around $k = 0$. (For interpretation of the references to colour in this figure legend, the reader is referred to the web version of this article.)

and v (see Eq. (40)) and $v_D = k/\sqrt{k^2 + m^2}$ the automaton and the Dirac drift coefficients. The bound in Eq. (30) explicitly quantifies the similarity between the evolution described by the automaton of Eq. (19) and the evolution described by the Dirac equation. Moreover, this result is exact (i.e. it does not depend on any approximations), easily computable (it is an explicit function of $m, \bar{k}, \bar{N}, t$), and provide an experimentally meaningful numerical value (since p_e is the probability of an experiment).

A simplified version of the bound in the $k, m \ll 1$ regime can be obtained by expanding in series the function g in Eq. (31) near $m = \bar{k} = 0$. Truncating the expansion at the leading order and neglecting a small constant term we have

$$g(m, \bar{k}, \bar{N}, t) \approx \frac{1}{6} m^2 \bar{k} \, \bar{N} \, t. \tag{32}$$

By putting $\bar{p}_e = 0$, corresponding to $g(m, \bar{k}, \bar{N}, t) = \pi/2$, we obtain the minimum time required for discriminating perfectly between the automaton and the Dirac evolution

$$t_{\min}(m, \bar{k}, \bar{N}) \approx 3\pi \, \frac{1}{m^2 \bar{k} \bar{N}}. \tag{33}$$

Notice that this is an in-principle result, without any specification of the actual apparatus needed to achieve it. For a proton with $\bar{k} = k_{CR} \approx 10^{-8}$ (as for order of magnitude, we consider numerical values corresponding to ultra high energy cosmic rays (UHECR) [68]) we have

$$t_{\min}(m_p, k_{CR}, 1) \approx 3\pi \, 10^{46} \quad \text{Planck times} \approx 10^3 \text{ s}. \tag{34}$$

The consistency of our result can be checked by power expanding the Hamiltonian of Eq. (21) and the dispersion relation of Eq. (22) in the limit of $k, m \to 0$,

$$\mathbf{H}_A(k) \simeq \mathbf{H}_D(k) + \frac{m}{3} \begin{pmatrix} mk & \frac{1}{2}(k^2 + m^2) \\ \frac{1}{2}(k^2 + m^2) & -mk \end{pmatrix}$$

$$\omega_A \simeq \omega_D \left(1 - \frac{m^2}{6} \frac{k^2 - m^2}{k^2 + m^2}\right) \qquad \omega_D := \omega_D(k, m) = \sqrt{k^2 + m^2} \tag{35}$$

and see that the leading terms are the Dirac Hamiltonian and the usual relativistic dispersion relation (see also Fig. 3).

The result of this section supports our interpretation of the parameters k and m of the automaton with the momentum and the mass of the Dirac field, respectively. Since the typical rest masses and momenta of particle physics experiments are many order of magnitude smaller than the Planck mass and the Planck momentum also the approximations (32) and (35) are justified.

One can say that the bound (30) extends "outside the limit" the results of Refs. [39,42,43] which compared the quantum walks model with the Dirac equations. Here we also have the additional bonuses that the many particle case is included and that the bound is explicitly written in terms of physical quantities like momentum, mass and number of the particle and is given in terms of an experimental meaningful quantity, i.e. the probability of error in a quantum channels discrimination procedure.

4. The one particle-sector of the Dirac automaton

In this section we explore the behavior of one particle states of the Dirac QCA. In particular we will consider initial states whose momentum distribution is smoothly peaked around some k_0, namely

$$|\psi(0)\rangle = \int_{-\pi}^{\pi} \frac{dk}{\sqrt{2\pi}} g(k,0)|s\rangle_k |k\rangle, \quad s = \pm, \tag{36}$$

where $g(k,0) \in C_0^\infty[-\pi, \pi]$ is a smooth function satisfying the bound

$$\frac{1}{2\pi} \int_{k_0-\sigma}^{k_0+\sigma} dk \, |g(k,0)|^2 \geq 1 - \epsilon, \quad \sigma, \epsilon > 0, \tag{37}$$

and the two-component vector $|s\rangle_k$ is defined in Eq. (23).

At time t and in the position representation, the state in Eq. (36) can be written as

$$|\psi(t)\rangle = \sum_x |\psi(x,t)\rangle |x\rangle \qquad |\psi(x,t)\rangle := e^{i(k_0 x - s\omega_0 t)} |\phi(x,t)\rangle$$

$$|\phi(x,t)\rangle := \int_{-\pi}^{\pi} \frac{dk}{\sqrt{2\pi}} e^{i(Kx - s\Omega(k,m)t)} g(k,0)|s\rangle_k \tag{38}$$

where we posed $K = k - k_0$ and $\Omega(k,m) = \omega(k,m) - \omega_0$, with $\omega_0 = \omega(k_0,m)$. It is convenient to take x, t to be real-valued continuous variable by extending the Fourier transform in Eq. (38) to real x, t. We derive the integral in Eq. (38) with respect to t, and expand Ω vs. k around k_0 up to the second order. Then, taking the resulting derivatives with respect to x out of the integral (using the dominated derivative theorem), we obtain the following dispersive differential equation with drift

$$i\partial_t |\tilde{\phi}(x,t)\rangle = s \left(iv \frac{\partial}{\partial x} - \frac{1}{2} D \frac{\partial^2}{\partial x^2} \right) |\tilde{\phi}(x,t)\rangle, \tag{39}$$

with the drift constant v and the diffusion constant D depending on k and m as follows

$$v := \sqrt{\frac{1-m^2}{1+m^2 \cot^2(k_0)}}, \qquad D := \frac{\sqrt{1-m^2}\, m^2 \cos(k_0)}{(\sin^2(k_0) + m^2 \cos^2(k_0))^{\frac{3}{2}}}, \tag{40}$$

and with the identification of the initial condition $|\tilde{\phi}(x,0)\rangle = |\phi(x,0)\rangle$.

The drift and diffusion coefficients are obtained as derivatives of the dispersion relation as $v = \omega_{k_0}^{(1)}$ and $D = \omega_{k_0}^{(2)}$, where

$$\omega_{k_0}^{(n)} = \left. \frac{\partial^n \omega(k,m)}{\partial k^n} \right|_{k_0}. \tag{41}$$

For $|\psi(x, 0)\rangle$ satisfying Eq. (37), Eq. (39) provides the approximation of the state of the particle $|\tilde{\psi}(x, t)\rangle = e^{i(k_0 x - s \omega_0 t)}|\tilde{\phi}(x, t)\rangle$, corresponding to

$$|\tilde{\psi}(t)\rangle = \int_{-\pi}^{\pi} \frac{\mathrm{d}k}{\sqrt{2\pi}} e^{-is\left(\omega_0 + vk - \frac{1}{2}Dk^2\right)t} g(k, 0)|s\rangle_k |k\rangle. \tag{42}$$

The accuracy of this approximation can be quantified in terms of the parameters σ and ϵ of the initial state by evaluating (see Appendix C) the overlap between the states (38) and (42)

$$|\langle \tilde{\psi}(t)|\psi(t)\rangle| \geq 1 - \epsilon - \gamma \sigma^3 t - \mathcal{O}(\sigma^5)t, \quad \gamma = \frac{\omega_{k_0}^{(3)}}{2\pi} \int_{k_0 - \sigma}^{k_0 + \sigma} \mathrm{d}k |g(k, 0)|^2. \tag{43}$$

We can test the accuracy of the approximation by comparing it with the automaton simulation. In Fig. 4 we show an example where the initial state (36) is a superposition of Hermite functions (the polynomials $H_j(x)$ multiplied by the Gaussian) peaked around a very high momentum $k_0 = 3\pi/10$ and for inertial mass $m = 0.6$. The mean value moves at the group velocity given by the drift coefficient v. One can notice how the approximation remains accurate even for small position spreads of few Planck lengths. For a spread $\hat{\sigma}$ of the order of a Fermi as in a typical particle physics scenario, the time t needed for a significant departure would be comparable to many universe life-times.

In the relativistic regime $k, m \ll 1$ and $k/m \gg 1$, the dispersive differential equation (39) approaches the Dirac equation. The leading order and the corrections to the drift and diffusion coefficients introduced by the automaton evolution are

$$\begin{aligned} v &= \frac{k}{\sqrt{k^2 + m^2}} \left(1 - \frac{1}{3}m^2 + \frac{1}{6}\frac{m^2 k^2}{k^2 + m^2}\right), \\ D &= \frac{m^2}{\sqrt{(k^2 + m^2)^3}} \left(1 + \frac{1}{3}m^2 k^2 - \frac{1}{2}\frac{m^2 k^4}{k^2 + m^2}\right). \end{aligned} \tag{44}$$

The leading order in v and D correspond to the Dirac equation.

In the non relativistic regime, $k, m \ll 1$ and $k/m \ll 1$ the usual Schrödinger drift and diffusion coefficients are recovered with the following corrections

$$v = \frac{k}{m}\left(1 + \frac{1}{3}m^2\right), \qquad D = \frac{1}{m}\left(1 + \frac{5}{6}k^2\right). \tag{45}$$

Notice that the leading terms are just the usual group-velocity and diffusion coefficient of the Schrödinger equation.

The momentum dependent differential equation (39) along with the leading terms in the relativistic and non relativistic regimes (see Eqs. (44) and (45)) provides a useful analytic tool for evaluating the macroscopic evolution of the automaton, which otherwise would not be computable in practice. We now consider an elementary discrimination experiment between the Dirac automaton evolution and the usual Dirac one based on particle fly-time.

Consider again a proton UHECR with $m_p \approx 10^{-19}$ and momentum peaked around $k_{CR} \approx 10^{-8}$ in Planck units, with a spread σ. We ask what is the minimal time t_{CR} for observing a complete spatial separation between the trajectory predicted by the cellular automaton model and the one described by the usual Dirac equation. Thus we require the separation between the two trajectories to be greater than $\hat{\sigma} = \sigma^{-1}$ the initial proton's width in the position space. Notice that UHECR belong to the relativistic regime $m_p, k_{CR} \ll 1$, where the automaton well approximates the usual Dirac evolution. We describe the state evolution of the wave-packet of the proton using the differential equation (39) for an initial Gaussian state. The Dirac evolution corresponds to the differential equation (39) with drift and diffusion coefficients given by the leading-order terms in Eq. (44), whereas the automaton is described by the full expansion. Taking the difference between the drift coefficient in the two cases one can evaluate the time required to have a separation $\hat{\sigma}$ between the automaton and the Dirac particle
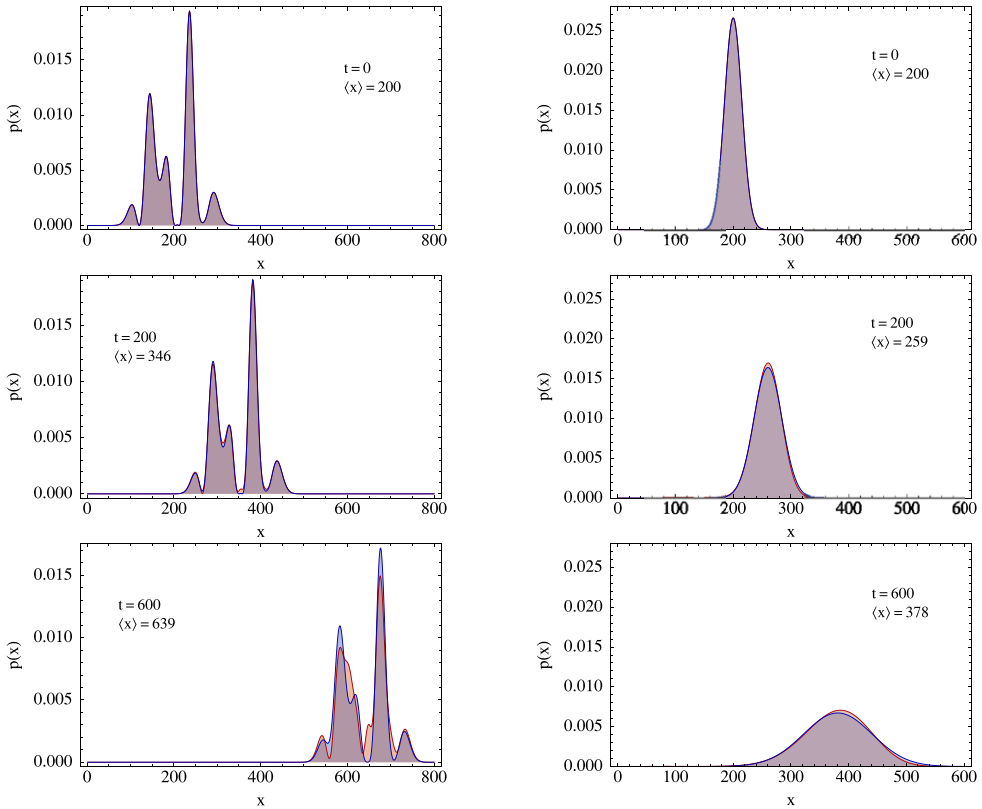
Fig. 4. Test of the approximation (42) of the Dirac automaton evolution of Eq. (19) in one space dimension. Left figure: here the state (36) is a superposition of Hermite functions (the polynomials $H_j(x)$ multiplied by the Gaussian) peaked around momentum $k_0 = 3\pi/10$, specifically $|\psi(x, 0)\rangle = \mathcal{A}e^{ik_0x}\sum_{j\in\mathbb{N}} c_j e^{-x^2/4\hat{\sigma}^2} H_j(x/2\hat{\sigma})|+\rangle_{k_0}$ where $\hat{\sigma} = \sigma^{-1} = 20$ is the position variance corresponding to the momentum variance σ, and the nonvanishing terms are $c_0 = \sqrt{1/3}$, $c_2 = \sqrt{4/9}$, $c_7 = \sqrt{2/9}$. The automaton mass is $m = 0.6$. The momentum and mass parameters are in the Planckian ultrarelativistic regime. In the picture we show a comparison at three different times $t = 0$, $t = 200$ and $t = 600$ between the automaton probability distribution $|\psi(x, t)|^2$ (in red) and the solution of the differential equation (39) $|\tilde{\psi}(x, t)|^2$ (in blue). The drift and diffusion coefficients are respectively $v = 0.73$ and $D = 0.31$. The mean position moves at the group velocity given by the drift coefficient v. The approximation remains accurate even for position spread $\hat{\sigma} = 20$ Planck lengths. According to Eq. (43) one has significant deviations for $t \approx \gamma\sigma^3$, which is $t = 600$ in the present case. However, a reasonable spread $\hat{\sigma}$ in a typical particle physics scenario is the Fermi length $\hat{\sigma} \approx 10^{20}$, that would need a time t comparable to many universe life-times to introduce a significant error. The ϵ error in Eq. (43) can be taken very small by considering $n\sigma$ instead of σ in Eq. (37). For Gaussian states it is enough to consider 3σ to get $\epsilon \approx 10^{-3}$. Right figure: The same three time comparison for the automaton $m = 0.4$, and an initial Gaussian state having width $\hat{\sigma} = \sigma^{-1} = 10$ and peaked around the momentum $k_0 = 0.1$. In this case the drift velocity and the diffusion coefficient are respectively $v = 0.22$ and $D = 2.30$. (For interpretation of the references to colour in this figure legend, the reader is referred to the web version of this article.)

$$t \approx \hat{\sigma}\left|\frac{6\sqrt{(k^2 + m^2)^3}}{m^2k^2(2m^2 + k)}\right|, \tag{46}$$

that, since it is $m_p/k_{CR} \ll 1$, further simplifies as follows

$$t_{CR} \approx 6\frac{\hat{\sigma}}{m_p^2}. \tag{47}$$

Furthermore, if we want the separation $\hat{\sigma}$ to be visible, the broadening $\hat{\sigma}_{br}(t)$ of the two packets must be much smaller than $\hat{\sigma}$. Using Eq. (44) one has

$$\hat{\sigma}_{br}(t) = \hat{\sigma} \left(\sqrt{1 + \left(\frac{D}{2\hat{\sigma}^2}t\right)^2} + \sqrt{1 + \left(\frac{D_D}{2\hat{\sigma}^2}t\right)^2} - 2 \right) \approx 2\hat{\sigma} \left(\sqrt{1 + \frac{m_p^4}{4\hat{\sigma}^4 k_{CR}^6}t^2} - 1 \right)$$

where $D_D = m^2(k^2 + m^2)^{-3/2}$ and we used $m_p/k_{CR} \ll 1$. From Eq. (47) we see that $\hat{\sigma} \gg \hat{\sigma}_{br}$ when

$$\hat{\sigma} \gg (k_{CR})^{-3} = 10^{22} \text{ Planck lengths} = 10^2 \text{ fm.} \tag{48}$$

With $\hat{\sigma} = 10^2$ fm (that is reasonable for a proton wave-packet) the flying time request for complete separation between the two trajectories is

$$t_{CR} \approx 6 \times 10^{60} \text{ Planck times} \approx 10^{17} \text{ s,} \tag{49}$$

that is comparable with the age of the universe and then incompatible with a realistic setup. We notice that UHECR, despite being very energetic, are very rare events and it is not possible to consider experiments involving more that one cosmic ray. Alternatively one could consider experiments involving many less energetic particles, reducing the minimal time for the discrimination according to the theoretical optimal result of Eq. (33), or experiments based on quantum interferometry and/or ultra-cold atoms as in Refs. [12,69–71].

5. Conclusions

In this paper we have considered the evolution of a quantum field in one dimension via a QCA. The automaton provides the one-step evolution of the fields located at the sites $x \in \mathbb{Z}$ of the lattice, inducing a discrete causal network of points (x, t). The Dirac automaton proposed in Ref. [17] is here derived as the minimum-dimension QCA holding the symmetries of the causal network, namely the parity and the time reversal invariance. The present one dimensional automaton is different from the *coined-quantum walk*, also known as generalized *Hadamard walk*, which is usually considered in the QWs literature.

The Dirac automaton, which depends on one parameter $m \in [0, 1]$ and has a band-limited wave-vector space $k \in [0, \pi]$, is shown to recover the Dirac equation in the limit of small k and m, which are then interpreted as the momentum and the mass of the Dirac field. We proved this result by considering the problem of discriminating between the Dirac QCA and the usual Dirac evolution for initial states with limited momentum and number of particles. We derived an exact lower bound for the probability of error in the discrimination, which is an explicit function of the mass of the field, the number and the momentum of the particles, and the duration of the evolution. We observe that for values of these parameters compatible with current experiments of particle physics the probability of error approaches $1/2$ (i.e. the two evolutions are indistinguishable). We stress that this analysis has not been obtained by taking the continuous limit of the lattice, namely taking the limit of a sequence of automata with smaller and smaller lattice spacing.

We have then derived an analytical approximation of the automaton evolution in terms of a dispersive differential equation. The approximation works for quantum states smoothly peaked around some momentum eigenvectors of the automaton with the drift and diffusion coefficients corresponding to the usual Dirac ones for small masses and momenta, in accordance to the above rigorous Dirac limit of the automaton.

In the paper [63], which is subsequent to the present one, the derivation of the Dirac QCA has been developed in the $2 + 1$ and in $3 + 1$ dimensional cases. One could extend the analysis of this paper to the automata of Ref. [63] considering the discrimination with their usual Dirac counterparts and evaluating the corresponding dispersive differential equation.

Up to now we have only considered the free field evolution. However, the physical interpretation of the automaton dispersion relation and wave-vector as energy and momentum needs the development of an interacting model. Moreover, as we stressed in the introduction, the analysis of this paper considers a fixed reference frame and a major point of the forthcoming research will be the study of relative reference frames within the QCA framework and of the analysis of the emerging notion of spacetime.

Acknowledgments

Appendix A. Derivation of the Dirac automaton

In this appendix we present in detail the derivation of the Dirac automaton (19), here reported in the momentum representation (see also Eq. (20))

$$\mathbf{U}(k) = \sum_{x \in \{-1,0,1\}} \mathbf{U}_x e^{-ikx}, \tag{A.1}$$

$$\mathbf{U}_1 = \begin{pmatrix} n & 0 \\ 0 & 0 \end{pmatrix}, \qquad \mathbf{U}_{-1} = \begin{pmatrix} 0 & 0 \\ 0 & n \end{pmatrix}, \qquad \mathbf{U}_0 = \begin{pmatrix} 0 & im \\ im & 0 \end{pmatrix}, \qquad n, m \in \mathbb{R}^+, \ n^2 + m^2 = 1, \tag{A.2}$$

starting from the assumptions (i)–(v) of Section 2. According to assumption (v) we show that for the internal dimension $\Lambda = 1$ there are not admissible non trivial (non-identical) automata. Then we show that for $\Lambda = 2$ there exist non trivial solutions and that they are all unitarily equivalent to the one given in Eq. (19). Here, for convenience of the reader, we report the unitarity conditions (see Eq. (16))

$$\mathbf{U}_1 \mathbf{U}_1^\dagger + \mathbf{U}_{-1} \mathbf{U}_{-1}^\dagger + \mathbf{U}_0 \mathbf{U}_0^\dagger = I, \tag{A.3}$$

$$\mathbf{U}_0 \mathbf{U}_1^\dagger + \mathbf{U}_{-1} \mathbf{U}_0^\dagger = 0, \tag{A.4}$$

$$\mathbf{U}_{-1} \mathbf{U}_1^\dagger = 0, \tag{A.5}$$

and the parity and time reversal covariance condition (see Eqs. (17) and (18))

$$\mathbf{P} \mathbf{U}_{\pm 1} \mathbf{P}^\dagger = \mathbf{U}_{\mp 1}, \qquad \mathbf{P} \mathbf{U}_0 \mathbf{P}^\dagger = \mathbf{U}_0, \tag{A.6}$$

$$\mathbf{T} \mathbf{U}_{\pm 1} \mathbf{T}^\dagger = \mathbf{U}_{\mp 1}^\dagger, \qquad \mathbf{T} \mathbf{U}_0 \mathbf{T}^\dagger = \mathbf{U}_0^\dagger, \tag{A.7}$$

for some unitary $\mathbf{P}$ and anti-unitary $\mathbf{T}$ operators.[9]

A.1. $\Lambda = 1$

For $\Lambda = 1$, the transition matrices are just complex numbers, say

$$\mathbf{U}_1 = e^{i\theta}, \qquad \mathbf{U}_{-1} = e^{i\theta'}, \qquad \mathbf{U}_0 = e^{i\theta''}. \tag{A.8}$$

In this case the unitarity constraints Eqs. (A.3), (A.4), and (A.5) lead to only three possible solutions

$$\mathbf{U}_1 = e^{i\theta}, \mathbf{U}_0 = \mathbf{U}_{-1} = 0, \qquad \mathbf{U}_{-1} = e^{i\theta}, \mathbf{U}_0 = \mathbf{U}_1 = 0, \qquad \mathbf{U}_0 = e^{i\theta}, \mathbf{U}_1 = \mathbf{U}_{-1} = 0, \tag{A.9}$$

with $\theta \in [0, 2\pi]$. Modulo a global phase, the above solutions correspond respectively to the right-shift ($\mathbf{U} = S_1$), the left-shift ($\mathbf{U} = S_{-1}$) and the identical ($\mathbf{U} = I$) automaton. Since in the right- and the left-shift solutions only one of the two transition matrices $\mathbf{U}_1$, $\mathbf{U}_{-1}$ is not null, parity covariance (A.7) cannot be satisfied and we are left with the trivial solution corresponding to the identical automaton.

---

[9] Any anti-unitary operator $\mathbf{T}$ is given by $\mathbf{T} = \mathbf{CU}$, where $\mathbf{U}$ is a unitary operator and $\mathbf{C}$ is the complex *conjugation operator* (given a basis $\{|\alpha_i\rangle\}$ of a Hilbert space $\mathcal{H}$ and an arbitrary vector $|\alpha\rangle = \sum c_i |\alpha_i\rangle$ it is $\mathbf{C}(\sum_i c_i |\alpha_i\rangle) = \sum_i c_i^* |\alpha_i\rangle$). Here we briefly recall the reason why the time reversal symmetry $\mathbf{T}$, interchanging the forward and backward light-cones $(t, x) \rightarrow (-t, x)$, cannot be represented by a unitary but by an anti-unitary operator. Take an eigenstate of the automaton $|s\rangle_k$, with $\mathbf{U}(k)|s\rangle_k = e^{i\mathbf{H}(k)}|s\rangle_k = e^{-is\omega}|s\rangle_k$, and consider the two states $|\psi\rangle_1 = \mathbf{T} e^{-is\omega t}|s\rangle_k$ and $|\psi\rangle_2 = e^{is\omega t}\mathbf{T}|s\rangle_k$. In the first case the state is evolved forward in time and then the time reversal is applied, in the second case we first act with the time-reversal operator and then evolve backward in time the state. If $\mathbf{T}$ is a symmetry of the Dirac theory the two operations must commute and one gets $|\psi\rangle_1 = |\psi\rangle_2 \Rightarrow \mathbf{T} e^{-is\omega t}|s\rangle_k = e^{is\omega t}\mathbf{T}|s\rangle_k$, which shows the non-linear action of the $\mathbf{T}$ operator.

A.2. $\Lambda = 2$

For $\Lambda = 2$ the three transition matrices can be generally parametrized as follows

$$\mathbf{U}_1 = \begin{pmatrix} a & b \\ c & d \end{pmatrix}, \qquad \mathbf{U}_{-1} = \begin{pmatrix} a' & b' \\ c' & d' \end{pmatrix}, \qquad \mathbf{U}_0 = \begin{pmatrix} x & y \\ z & w \end{pmatrix}, \tag{A.10}$$

with all entries arbitrary complex numbers.

Now we can fix the basis where $\mathbf{P}$ and $\mathbf{T}$ in Eqs. (A.6) and (A.7) are represented as

$$\mathbf{P} = \begin{pmatrix} 0 & 1 \\ 1 & 0 \end{pmatrix}, \qquad \mathbf{T} = \mathbf{C} \begin{pmatrix} 0 & 1 \\ 1 & 0 \end{pmatrix}, \tag{A.11}$$

where $\mathbf{C}$ is the anti-unitary operator denoting complex conjugation in the given representation. Indeed without loss of generality we can fix the representation (which fix a basis) for one of the two symmetries, say parity. Once parity is given we have to represent time reversal in the same basis, with different choices leading in general to non unitary equivalent solutions. However, assuming $[\mathbf{P}, \mathbf{T}] = 0$ as it is in the usual QFT (we do not consider the more general scenario where the two operators do not commute), and discarding the trivial case where $\mathbf{T} \propto I$, we are left with the representation of Eq. (A.11).

In the representation (A.11) the parity covariance (A.6) of the automaton gives

$$\mathbf{U}_1 = \begin{pmatrix} a & b \\ c & d \end{pmatrix}, \qquad \mathbf{U}_{-1} = \begin{pmatrix} d & c \\ b & a \end{pmatrix}, \qquad \mathbf{U}_0 = \begin{pmatrix} x & y \\ y & x \end{pmatrix}, \tag{A.12}$$

while from the time time-reversal covariance (A.7) it follows

$$\mathbf{U}_1 = \begin{pmatrix} a & b \\ b & d \end{pmatrix}, \qquad \mathbf{U}_{-1} = \begin{pmatrix} d & b \\ b & a \end{pmatrix}, \qquad \mathbf{U}_0 = \begin{pmatrix} x & y \\ y & x \end{pmatrix}. \tag{A.13}$$

Eq. (A.6) shows that $\mathbf{U}_1$ and $\mathbf{U}_{-1}$ are unitarily equivalent (they are related by conjugation with the unitary operator $\mathbf{P}$), and from the condition $\mathbf{U}_{-1}\mathbf{U}_1^\dagger = 0$ in (A.5) it follows that they are both rank one. Accordingly, without loss of generality, we can always write the two transition matrices as follows

$$\mathbf{U}_1 = \begin{pmatrix} a & b \\ \eta a & \eta b \end{pmatrix}, \qquad \mathbf{U}_{-1} = \begin{pmatrix} \eta b & \eta a \\ b & a \end{pmatrix}, \tag{A.14}$$

for some $\eta \in \mathbb{C}$. Now we consider separately the two cases $\eta = 0$, and $\eta \neq 0$.

($\eta = 0$) From the time reversal invariance (18), more precisely from $\mathbf{T}\mathbf{U}_1\mathbf{T}^\dagger = \mathbf{U}_{-1}^\dagger$, it follows $b = 0$. Using this result the unitarity condition (A.4) gives the two equalities $xa^* = ax^* = 0$ and $ya^* + ay^* = 0$. Since the case $a = 0$ is trivial ($\mathbf{U}_1 = \mathbf{U}_{-1} = 0$) it follows $x = 0$ and $\Re(ay^*) = 0$. Finally, using the unitarity condition (16) we get $|a|^2 + |y|^2 = 1$ that, up to a global phase, gives the unique solution

$$\mathbf{U}(k) = \begin{pmatrix} n e^{ik} & -im \\ -im & n e^{-ik} \end{pmatrix}, \quad n, m \in \mathbb{R}, \ n^2 + m^2 = 1. \tag{A.15}$$

The constants n and m in the last equation can be chosen positive since a change in the relative sign is obtained by a unitary conjugation with the matrix $\begin{pmatrix} 0 & -i \\ i & 0 \end{pmatrix}$.

($\eta \neq 0$) Noticing that for Eq. (A.13) it must be $\eta a = b$ we have

$$\mathbf{U}_1 = \begin{pmatrix} b/\eta & b \\ b & \eta b \end{pmatrix}, \qquad \mathbf{U}_{-1} = \begin{pmatrix} \eta b & b \\ b & b/\eta \end{pmatrix}, \tag{A.16}$$

and using again the condition $\mathbf{U}_{-1}\mathbf{U}_1^\dagger = 0$ in (16), with $\mathbf{U}_{\pm 1}$ as in Eq. (A.16), we get the constraints

$$|b|^2(\eta/\eta^* + 1) = |b|^2(\eta + \eta^*) = 0. \tag{A.17}$$

Since the case $b = 0$ is trivial, we take $b \neq 0$ in which case (A.17) implies $\Re(\eta) = 0$, say

$$\mathbf{U}_1 = \begin{pmatrix} -ib/\xi & b \\ b & i\xi b \end{pmatrix}, \qquad \mathbf{U}_{-1} = \begin{pmatrix} i\xi b & b \\ b & -ib/\xi \end{pmatrix}, \tag{A.18}$$

for some $\xi \in \mathbb{R}$ and with $\xi \neq 0$. Using the unitarity conditions (A.3) and (A.4) we get respectively the equalities

$$|x|^2 + |y|^2 + |b|^2(1 + \xi^2 + 1/\xi^2) = 1, \tag{A.19}$$

$$xy^* + yx^* = 0, \tag{A.20}$$

and

$$yb^* - by^* = yb^* + by^* = 0 \tag{A.21}$$

$$xb^* + bx^* = xb^* + \xi^2 bx^* = 0. \tag{A.22}$$

Since Eq. (A.21) implies both $y = pb$ and $y = iqb$ for some $p, q \in \mathbb{R}$, and $b \neq 0$ by hypothesis, it must be $y = 0$. Moreover, due to Eq. (A.20) which gives $x = iry$ for some $r \in \mathbb{R}$, we get $x = 0$ proving that the transition matrix $\mathbf{U}_0$ is the null matrix. Using Eq. (A.19) we find

$$\frac{(\xi^2 + 1)^2}{\xi^2}|b|^2 = 1 \Rightarrow b = e^{i\theta}\frac{\xi}{\xi^2 + 1} \tag{A.23}$$

with $\theta \in \mathbb{R}$ and the general solution for $\eta \neq 0$, up to a global phase, is finally given by

$$\mathbf{U}(k) = \begin{pmatrix} i\dfrac{\xi^2}{\xi^2 + 1}e^{ik} - i\dfrac{1}{\xi^2 + 1}e^{-ik} & \dfrac{\xi}{\xi^2 + 1}(e^{ik} + e^{-ik}) \\ \dfrac{\xi}{\xi^2 + 1}(e^{ik} + e^{-ik}) & i\dfrac{\xi^2}{\xi^2 + 1}e^{-ik} - i\dfrac{1}{\xi^2 + 1}e^{ik} \end{pmatrix}. \tag{A.24}$$

Now we observe that the dispersion relation of the solutions (A.15) and Eq. (A.24), corresponding respectively to the cases $\eta = 0$ and $\eta \neq 0$, are given by

$$\omega_{\eta=0}(k) = \arccos(n\cos(k)), \qquad \omega_{\eta\neq0}(k) = \arccos\left(\frac{\xi^2-1}{\xi^2+1}\cos(k)\right), \tag{A.25}$$

which coincide upon the identification $n = \frac{\xi^2-1}{\xi^2+1}$ (this is always possible because both n and $\frac{\xi^2-1}{\xi^2+1}$ are real numbers smaller or equal to one). Since the automata in Eqs. (A.15) and (A.24) have the same dispersion relation they have the same eigenvalues $e^{\pm i\omega}$ and are then unitarily equivalent.

Appendix B. Proof of the bound (30)

In this appendix we detail the proof of the bound (30) in Section 3 which provides the probability of optimal error probability in discriminating the Dirac automaton and the usual Dirac evolution. The discrimination experiment can have a generic duration t and the unitary operators to be discriminated are explicitly given by

$$\mathbf{U}^t(k) = \exp(-i\mathbf{H}(k)t) = \begin{pmatrix} \cos(\omega t) + i\dfrac{\sin(\omega t)}{\omega}a & -ib\dfrac{\sin(\omega t)}{\omega} \\ -ib\dfrac{\sin(\omega t)}{\omega} & \cos(\omega t) - i\dfrac{\sin(\omega t)}{\omega}a \end{pmatrix} \tag{B.1}$$

$$a := \frac{\omega}{\sin(\omega)}n\sin(k) \qquad b := \frac{\omega}{\sin(\omega)}m$$

$$\mathbf{U}_D^t(k) = \exp(-i\mathbf{H}_D(k)t) = \begin{pmatrix} \cos(\lambda t) + i\dfrac{\sin(\lambda t)}{\lambda}k & -im\dfrac{\sin(\lambda t)}{\lambda} \\ -im\dfrac{\sin(\lambda t)}{\lambda} & \cos(\lambda t) - i\dfrac{\sin(\lambda t)}{\lambda}k \end{pmatrix}, \tag{B.2}$$

as can be easily verified by direct computation using the Hamiltonians in Eqs. (21) and (25). The proof of the bound (30) goes through the following three lemmas.

Lemma 1. *Let $\mathbf{U}_D^t(k)$ and $\mathbf{U}^t(k)$ be defined according to Eqs.* (B.1), (B.2) *and let us define* $\mathbf{V}(k,t) = \mathbf{U}_D^t(k)\mathbf{U}^{t\dagger}(k)$. *Let $e^{i\mu(k,m,t)}$ be an eigenvalue of $\mathbf{V}(k,t)$. Then the following bound holds:*

$$\cos(\mu(k,m,t)) \geq \cos(\alpha t) - \beta \tag{B.3}$$

where

$$\alpha(k,m) := \omega_D - \omega$$
$$\beta(k,m) := \frac{1}{2}\left(1 - vv_D - \sqrt{(1-v^2)(1-v_D^2)}\right). \tag{B.4}$$

Proof. Since both $\mathbf{U}_D^t(k)$ and $\mathbf{U}^{t\dagger}(k)$ are $SU(2)$ matrices, we have that $\mathbf{V}(k,t)$ is an $SU(2)$ matrix and its eigenvalues must be of the form $e^{i\mu(k,m,t)}$ and $e^{-i\mu(k,m,t)}$. This implies the equality $\cos(\mu(k,m,t)) = \frac{1}{2}\mathrm{Tr}[\mathbf{V}(k,t)]$ which by direct computation gives

$$\cos(\mu(k,m,t)) = \left(1 - \frac{\beta}{2}\right)\cos(\alpha t) + \frac{\beta}{2}\cos(\gamma t) \tag{B.5}$$

where α and β are defined accordingly with Eq. (B.4) and $\gamma := \omega + \omega_D$. Finally, from Eq. (B.5) one has the bound $\cos(\mu(k,m,t)) \geq \cos(\alpha t) - \beta$. ■

The second lemma shows the monotonicity of the two functions α, β in Lemma 1:

Lemma 2. *Let $\alpha(k,m)$ and $\beta(k,m)$ be defined as in Eq.* (B.4) *and $0 \leq \bar{k} < \pi$. Then we have*

$$\bar{\alpha} := \max_{k \in [-\bar{k},\bar{k}]} |\alpha| = \max_{k \in \{0,\bar{k}\}} |\alpha|$$
$$\bar{\beta} := \max_{k \in [-\bar{k},\bar{k}]} |\beta| = \max_{k \in \{0,\bar{k}\}} |\beta| \quad \forall m \in [0,1]. \tag{B.6}$$

Proof. Since both ω and ω_D are even functions of k, from Eq. (B.4) we have that also α and β are even function of k. For this reason we can restrict to $k \in [0, \bar{k}]$. The equality (B.6) can be proved by showing that α and β are nondecreasing functions of k for $k \in [0, \bar{k}]$.

Since $\partial_k \alpha = v_D - v$, clearly $v_D^2 - v^2 \geq 0$ for $k \in [0, \pi)$ implies $\partial_k \alpha \geq 0$ in the same interval. By direct computation one can verify that

$$(v_D)^2 - (v)^2 = \frac{x(k,m)}{y(k,m)} \tag{B.7}$$

$$x(k,m) := k^2 - \sin^2(k)(1-m^2) \tag{B.8}$$

$$y(k,m) := (k^2 + m^2)(\sin^2(k) + m^2\cos^2(k)). \tag{B.9}$$

Clearly we have $y(k,m) \geq 0$ and since $k \geq \sin(k)$ for $0 \leq k < \pi$, the thesis is proved.

Again the monotonicity of β for $k \in [0, \pi)$ follows from $\partial_k \beta \geq 0$ in the same interval. By elementary computation we have

$$\partial_k \beta = x(k,m)y(k,m)z(k,m) \tag{B.10}$$

$$x(k,m) := \frac{m^2}{\omega_D \sin^2(\omega)} \tag{B.11}$$

$$y(k,m) := (n\sin(k) - k) \tag{B.12}$$

$$z(k,m) := \frac{n\cos(k)}{\sin^2(\omega)} - \frac{1}{\omega_D^2}. \tag{B.13}$$

Clearly $x(k, m)y(k, m) \leq 0$ for $k \in [0, \pi)$ and we just have to verify that $z(k, m) \leq 0$ in that interval, namely

$$m^2 \cos^2(k) + \sin^2(k) - n \cos(k)\omega_D^2 \geq 0. \tag{B.14}$$

The last equation is clearly satisfied for $k \in [\pi/2, \pi]$ therefore we restrict to $k \in [0, \pi/2]$. This allows to divide the left side of Eq. (B.14) by $\cos(k)$ achieving

$$m^2 \cos(k) + \frac{\sin^2(k)}{\cos(k)} - n\omega_D^2 \geq 0 \tag{B.15}$$

which is satisfied if

$$w(k, m) := m^2 \cos(k) + \sin^2(k) - n\omega_D^2 \geq 0. \tag{B.16}$$

It is easy to see that, for any $m \in [0, 1]$, we have $\left(\partial_k^{(i)} w(k, m) \right)_{k=0} = 0$ for $i = 0, 1$, while $\partial_k^{(2)} f(k, m) \geq 0$ for any $k \in [0, \pi/2]$, which gives the monotonicity of β. ∎

Lemma 3. *Let* $0 \leq \bar{k} < \pi$, $\bar{N}$ *be a positive integer number, and* $\bar{\alpha}$, $\bar{\beta}$ *be defined as in Eq.* (B.6). *If* $\bar{\beta} \leq 1 - \cos(\frac{\pi}{2\bar{N}})$ *and* $t \leq f(\bar{k}, m, \bar{N})$ *where*

$$f(\bar{k}, m, \bar{N}) := \frac{\arccos\left(\cos\left(\frac{\pi}{2\bar{N}} \right) + \bar{\beta} \right)}{\bar{\alpha}} \tag{B.17}$$

then

$$\bar{N}\mu(k, m, t) \leq g(\bar{k}, m, \bar{N}, t) \leq \frac{\pi}{2} \tag{B.18}$$

where $g(\bar{k}, m, \bar{N}, t) := \bar{N} \arccos\left(\cos(\bar{\alpha}t) - \bar{\beta} \right)$.

Proof. The conditions $t \leq f(\bar{k}, m, \bar{N})$ and $\bar{\beta} \leq 1 - \cos(\frac{\pi}{2\bar{N}})$ imply

$$0 \leq \bar{\alpha}t \leq \arccos\left(\cos\left(\frac{\pi}{2\bar{N}} \right) + \bar{\beta} \right) \Rightarrow 1 \geq \cos(\bar{\alpha}t) - \bar{\beta} \geq \cos\left(\frac{\pi}{2\bar{N}} \right)$$

$$\Rightarrow \cos(\alpha t) - \beta \geq \cos(\bar{\alpha}t) - \bar{\beta} \geq \cos\left(\frac{\pi}{2\bar{N}} \right). \tag{B.19}$$

By exploiting the bound (B.3) into Eq. (B.19) we have

$$\cos(\mu(k, m, t)) \geq \cos(\bar{\alpha}t) - \bar{\beta} \geq \cos\left(\frac{\pi}{2\bar{N}} \right) \Rightarrow \bar{N}\mu(k, m, t)$$

$$\leq \bar{N} \arccos\left(\cos(\bar{\alpha}t) - \bar{\beta} \right) \leq \frac{\pi}{2}. \quad ∎ \tag{B.20}$$

We are now ready to prove the bound (30).

Proposition 1. *Let* U^t *and* U_D^t *be the unitary evolutions given by the Dirac QCA and by the Dirac equation respectively. If the hypothesis of Lemma 3 holds we have*

$$\sup_{\rho \in \mathcal{T}_{\bar{k},\bar{N}}} \|(U^t \rho U^{t\dagger} - U_D^t \rho U_D^{t\dagger})\|_1 \leq \sqrt{1 - \cos^2(g(\bar{k}, m, \bar{N}, t))}. \tag{B.21}$$

Proof. First we notice that thanks to the convexity of the trace distance we can without loss of generality consider ρ to be pure. If ρ is a pure state $|\chi\rangle\langle\chi|$ the trace distance becomes $\sqrt{1 - |\langle\chi|U^t U_D^{t\dagger}|\chi\rangle|^2} = \sqrt{1 - |\langle\chi|V(t)|\chi\rangle|^2}$. If we expand $|\chi\rangle$ on a basis of eigenstates of V, i.e. $|\chi\rangle = \sum_{N,\mathbf{k},\mathbf{s}} \sqrt{p_{N,\mathbf{k},\mathbf{s}}}|N,\mathbf{k},\mathbf{s}\rangle$, we have

$$
|\langle\chi|V(t)|\chi\rangle| = \left| \sum_{N,\mathbf{k},\mathbf{s}} p_{N,\mathbf{k},\mathbf{s}} \exp\left(i \sum_{j=0}^{N} s_j \mu(k_j, m, t) \right) \right|
$$

$$
\geq \left| \sum_{N,\mathbf{k},\mathbf{s}} p_{N,\mathbf{k},\mathbf{s}} \cos\left(\sum_{j=0}^{N} s_j \mu(k_j, m, t) \right) \right|. \tag{B.22}
$$

By exploiting the bound (B.18) into Eq. (B.22) we have

$$
\left| \sum_{N,\mathbf{k},\mathbf{s}} p_{N,\mathbf{k},\mathbf{s}} \cos\left(\sum_{j=0}^{N} s_j \mu(k_j, m, t) \right) \right|^2 \geq \cos^2(g(\bar{k}, m, \bar{N}, t))
$$

which finally implies

$$
\sqrt{1 - |\langle\chi|V(t)|\chi\rangle|^2} \leq \sqrt{1 - \cos^2(g(\bar{k}, m, \bar{N}, t))}. \quad \blacksquare
$$

Inserting the bound (B.21) into Eq. (28) we finally have the bound (30).

Appendix C. Derivation of Eq. (43)

Here we evaluate the overlap between the exact automaton evolution $|\psi(t)\rangle$ and the dispersive differential equation approximation $|\tilde{\psi}(t)\rangle$

$$
|\langle\tilde{\psi}(t)|\psi(t)\rangle| = \left| \int_{-\pi}^{\pi} \frac{dk}{2\pi} e^{-i(\omega_{k_0}^{(3)} k^3 + \mathcal{O}(k^4))t} |g(k,0)|^2 \right|
$$

$$
\geq \left| \frac{1}{2\pi} \int_{k_0-\sigma}^{k_0+\sigma} dk\, e^{-i(\omega_{k_0}^{(3)} k^3 + \mathcal{O}(k^4))t} |g(k,0)|^2 \right|
$$

$$
- \left| \frac{1}{2\pi} \int_{|k-k_0|\geq\sigma} dk\, e^{-i(\omega_{k_0}^{(3)} k^3 + \mathcal{O}(k^4))t} |g(k,0)|^2 \right|
$$

$$
\geq \left| 1 - it \frac{\omega_{k_0}^{(3)} \sigma^3}{2\pi} \int_{k_0-\sigma}^{k_0+\sigma} dk\, |g(k,0)|^2 - \mathcal{O}(\sigma^5)t \right| - \epsilon
$$

$$
\geq 1 - \epsilon - \gamma\sigma^3 t - \mathcal{O}(\sigma^5)t
$$

with the constant $\gamma = \frac{\omega_{k_0}^{(3)}}{2\pi} \int_{k_0-\sigma}^{k_0+\sigma} dk\, |g(k,0)|^2$.

References

[1] C. Rovelli, L. Smolin, Nuclear Phys. B 8 (1990) 80–152.
[2] A. Ashtekar, C. Rovelli, L. Smolin, Phys. Rev. Lett. 69 (1992) 237–240.
[3] C. Rovelli, L. Smolin, Nuclear Phys. B 442 (1995) 593–619.
[4] L. Bombelli, J. Lee, D. Meyer, R. Sorkin, Phys. Rev. Lett. 59 (1987) 521.
[5] A. Connes, J. Lott, Nuclear Phys. B Proc. Suppl. 18 (1991) 29–47.
[6] H. Snyder, Phys. Rev. 71 (1947) 38–41.
[7] G. Amelino-Camelia, Internat. J. Modern Phys. D 11 (2002) 35–59.
[8] G. Amelino-Camelia, T. Piran, Phys. Rev. D 64 (2001) 036005.
[9] J. Magueijo, L. Smolin, Phys. Rev. D 67 (2003) 044017.
[10] C. Hogan, 2010. Arxiv Preprint arXiv:1002.4880.

[11] C. Hogan, 2012. Arxiv Preprint arXiv:1204.5948.
[12] I. Pikovski, M. Vanner, M. Aspelmeyer, M. Kim, C. Brukner, Nat. Phys. 331 (2012) 393–397.
[13] J.D. Bekenstein, Lett. Nuovo Cimento (1971–1985) 4 (1972) 737–740.
[14] S.W. Hawking, Comm. Math. Phys. 43 (1975) 199–220.
[15] G. D'Ariano, CP1232 Quantum Theory: Reconsideration of Foundations, vol. 5, 2010, p. 3. arXiv:1001.1088.
[16] G. D'Ariano, Advances in Quantum Theory, in: AIP Conf. Proc., vol. 1327, 2011, p. 7. arXiv:1012.0535.
[17] G.M. D'Ariano, Phys. Lett. A 376 (2011).
[18] G. D'Ariano, 2012. (arXiv:1211.2479).
[19] G.M. D'Ariano, Il Nuovo Saggiatore 28 (2012) 13.
[20] J. von Neumann, Theory of Self-Reproducing Automata, University of Illinois Press, Urbana, London, 1966.
[21] J. Watrous, 36th Annual Symposium on Foundations of Computer Science, Proceedings, IEEE, 1995, pp. 528–537.
[22] C. Durr, M. Santha, 37th Annual Symposium on Foundations of Computer Science, Proceedings, IEEE, 1996, pp. 38–45.
[23] C. Dürr, H. Lê Thanh, M. Santha, in: C. Puech, R. Reischuk (Eds.), STACS 96, in: Lecture Notes in Computer Science, vol. 1046, Springer, Berlin, Heidelberg, 1996, pp. 281–292.
[24] B.M. Boghosian, W. Taylor IV, Phys. Rev. E 57 (1998) 54.
[25] B.M. Boghosian, W. Taylor IV, Physica D 120 (1998) 30–42.
[26] P.J. Love, B.M. Boghosian, Quantum Inf. Process. 4 (2005) 335–354.
[27] B. Schumacher, R. Werner, 2004. Arxiv Preprint quant-ph/0405174.
[28] P. Arrighi, V. Nesme, R. Werner, J. Comput. System Sci. 77 (2011) 372–378.
[29] D. Gross, V. Nesme, H. Vogts, R. Werner, Comm. Math. Phys. (2012) 1–36.
[30] G. Grossing, A. Zeilinger, Complex Syst. 2 (1988) 197–208.
[31] Y. Aharonov, L. Davidovich, N. Zagury, Phys. Rev. A 48 (1993) 1687–1690.
[32] A. Ambainis, E. Bach, A. Nayak, A. Vishwanath, J. Watrous, Proceedings of the Thirty-Third Annual ACM Symposium on Theory of Computing, ACM, 2001, pp. 37–49.
[33] A.M. Childs, R. Cleve, E. Deotto, E. Farhi, S. Gutmann, D.A. Spielman, Proceedings of the Thirty-Fifth Annual ACM Symposium on Theory of Computing, ACM, 2003, pp. 59–68.
[34] A. Ambainis, SIAM J. Comput. 37 (2007) 210–239.
[35] F. Magniez, M. Santha, M. Szegedy, SIAM J. Comput. 37 (2007) 413–424.
[36] E. Farhi, J. Goldstone, S. Gutmann, 2007. ArXiv Preprint quant-ph/0702144.
[37] G. 't Hooft, Nuclear Phys. B 342 (1990) 471–485.
[38] S. Succi, R. Benzi, Physica D 69 (1993) 327–332.
[39] I. Bialynicki-Birula, Phys. Rev. D 49 (1994) 6920.
[40] D. Meyer, J. Stat. Phys. 85 (1996) 551–574.
[41] J. Yepez, Quantum Inf. Process. 4 (2006) 471–509.
[42] F.W. Strauch, Phys. Rev. A 73 (2006) 054302.
[43] F.W. Strauch, J. Math. Phys. 48 (2007) 082102.
[44] A.J. Bracken, D. Ellinas, I. Smyrnakis, Phys. Rev. A 75 (2007) 022322. http://dx.doi.org/10.1103/PhysRevA.75.022322.
[45] C.M. Chandrashekar, S. Banerjee, R. Srikanth, Phys. Rev. A 81 (2010) 062340. http://dx.doi.org/10.1103/PhysRevA.81.062340.
[46] G. Di Molfetta, F. Debbasch, J. Math. Phys. 53 (2012) 123302.
[47] P. Arrighi, V. Nesme, M. Forets, J. Phys. A: Math. Theor. 47 (2014) 465302.
[48] R. Feynman, Internat. J. Theoret. Phys. 21 (1982) 467–488.
[49] D. Deutsch, Proc. R. Soc. A 400 (1985) 97–117.
[50] T. Cao, S. Schweber, Synthese 97 (1993) 33–108.
[51] S. Auyang, How is Quantum Field Theory Possible? Oxford University Press, USA, 1995.
[52] P. Teller, An Interpretive Introduction to Quantum Field Theory, Princeton Univ. Pr., 1997.
[53] T. Cao, Conceptual Foundations of Quantum Field Theory, Cambridge Univ. Pr., 2004.
[54] R. Haag, D. Kastler, J. Math. Phys. 5 (1964) 848.
[55] R.F. Streater, A.S. Wightman, PCT, Spin and Statistics, and All That, Princeton University Press, 1964.
[56] J. Magueijo, L. Smolin, Phys. Rev. Lett. 88 (2002) 190403.
[57] A. Bibeau-Delisle, A. Bisio, G.M. D'Ariano, P. Perinotti, A. Tosini, 2013. ArXiv Preprint arXiv:1310.6760.
[58] H.B. Nielsen, M. Ninomiya, Phys. Lett. B 105 (1981) 219–223.
[59] D. Reitzner, D. Nagaj, V. Bužek, Acta Phys. Slovaca 61 (2011) 603–725. Reviews and Tutorials.
[60] P. Knight, E. Roldán, J. Sipe, J. Modern Opt. 51 (2004) 1761–1777.
[61] G. Valcárcel, E. Roldán, A. Romanelli, New J. Phys. 12 (2010) 123022.
[62] A. Ahlbrecht, H. Vogts, A. Werner, R. Werner, J. Math. Phys. 52 (2011) 042201.
[63] G.M. D'Ariano, P. Perinotti, Phys. Rev. A 90 (2014) 062106.
[64] A. Bisio, G.M. D'Ariano, A. Tosini, Phys. Rev. A 88 (2013) 032301.
[65] T. Toffoli, N. Margolus, Cellular Automata Machines, MIT Press, 1987.
[66] G. D'Ariano, P. Lo Presti, M. Paris, Phys. Rev. Lett. 87 (2001) 270404.
[67] C. Helstrom, Quantum Detection and Estimation Theory, Vol. 84, Academic Press, New York, 1976.
[68] M. Takeda, N. Hayashida, K. Honda, N. Inoue, K. Kadota, F. Kakimoto, K. Kamata, S. Kawaguchi, Y. Kawasaki, N. Kawasumi, et al., Phys. Rev. Lett. 81 (1998) 1163–1166.
[69] M. Moyer, Sci. Am. (2012).
[70] C. Hogan, Phys. Rev. D 85 (2012).
[71] G. Amelino-Camelia, C. Laemmerzahl, F. Mercati, G. Tino, Phys. Rev. Lett. 103 (2009) 171302.